HHS Public Access

Author manuscript

Clin Cancer Res. Author manuscript; available in PMC 2017 March 01.

Published in final edited form as:

Clin Cancer Res. 2016 March 1; 22(5): 1274–1283. doi:10.1158/1078-0432.CCR-15-1706.

Loss of glycogen debranching enzyme AGL drives bladder tumor growth via induction of hyaluronic acid synthesis

Sunny Guin[1,2], **Yuanbin Ru**[1,2,#], **Neeraj Agarwal**[1,2], **Carolyn R. Lew**[1,2], **Charles Owens**[1,2], **Giacomo P. Comi**[3], and **Dan Theodorescu**[1,2,4,*]

[1]Department of Surgery (Urology), University of Colorado, Denver, CO, USA

[2]Department of Pharmacology, University of Colorado, Denver, CO, USA

[3]IRCCS Foundation Ca' Granda Ospedale Maggiore Policlinico, Milan, Italy

[4]University of Colorado Comprehensive Cancer Center, Denver, CO, USA

Abstract

Purpose—We demonstrated that Amylo-alpha-1-6-glucosidase-4-alpha-glucanotransferase (AGL) is a tumor growth suppressor and prognostic marker in human bladder cancer. Here we determine how AGL loss enhances tumor growth, hoping to find therapeutically tractable targets/pathways that could be used in patients with low AGL expressing tumors.

Experimental Design—We transcriptionally profiled bladder cell lines with different AGL expression. By focusing on transcripts overexpressed as a function of low AGL and associated with adverse clinicopathologic variables in human bladder tumors, we sought to increase the chances of discovering novel therapeutic opportunities.

Results—One such transcript was hyaluronic acid synthase 2 (HAS2), an enzyme responsible for hyaluronic acid (HA) synthesis. HAS2 expression was inversely proportional to that of AGL in bladder cancer cells and immortalized and normal urothelium. HAS2 driven HA synthesis was enhanced in bladder cancer cells with low AGL and this drove anchorage dependent and independent growth. siRNA mediated depletion of HAS2 or inhibition of HA synthesis by 4-Methylumbelliferone (4MU) abrogated *in vitro* and xenograft growth of bladder cancer cells with low AGL. AGL and HAS2 mRNA expression in human tumors was inversely correlated in patient datasets. Patients with high HAS2 and low AGL tumor mRNA expression had poor survival lending clinical support to xenograft findings that HAS2 drives growth of tumors with low AGL.

Conclusion—Our study establishes HAS2 mediated HA synthesis as a driver of growth of bladder cancer with low AGL and provides preclinical rationale for personalized targeting of HAS2/HA signaling in patients with low AGL expressing tumors.

[*]Correspondence to: Dan Theodorescu, University of Colorado Comprehensive Cancer Center, Aurora, C0 80045, phone: (303)724-7135; FAX: (303)724-3162; dan.theodorescu@ucdenver.edu.

[#]Current address: BioMarin Pharmaceutical Inc., Novato, CA, USA

Authors' Contribution: Conception and design by DT and SG. Acquisition of data by SG, NA, CRL and CO. Analysis and interpretation of data by SG, NA, CRL, CO and DT. Microarray and statistical analysis and interpretation were conducted by YR. Writing, review and/or revision of the manuscript by SG, YR, CRL and DT.

Conflict of Interest: None

Keywords

AGL; HAS2; hyaluronic acid; bladder cancer; prognosis

INTRODUCTION

Amylo-alpha-1-6-glucosidase-4-alpha-glucanotransferase (AGL) and the three glycogen phosphorylase (PYG) isoforms are the enzymes responsible for glycogen breakdown (glycogenolysis) in humans. Mutational inactivation of AGL leads to buildup of abnormal glycogen in the liver, heart and skeletal muscle leading to Glycogen Storage Disease III (GSD III)(2, 3), a condition with good prognosis when treated by high protein and carbohydrate diet. While well characterized clinically, pathologically, genetically and metabolically, the low prevalence of GSD III has limited epidemiologic investigation to determine if such patients are at higher risk for other conditions.

In a recent study we used a whole genome lentiviral shRNA based *in vivo* screen to discover new tumor growth suppressors(4). This work identified AGL as a tumor growth suppressor and prognostic marker in human bladder cancer, for the first time assigning to AGL a role in cancer biology(4). We further showed that both wild type and enzymatically inactive variants of AGL can inhibit growth of cancer cells suggesting that in cancer, unlike in GSD III, AGL works non-enzymatically to exert its growth effects(4). Further demonstrating that AGL suppresses growth by such “moonlighting” or glycogenolysis independent mechanisms, was finding that loss of PYG, unlike that of AGL, did not promote growth of human bladder cancer cell lines(4).

Metabolomic profiling showed that bladder cancer cells with low AGL are more dependent on extracellular glucose and SHMT2 mediated glycine synthesis for proliferation(4). While mechanistically insightful, this analysis did not provide any therapeutically tractable targets or pathways that could be used in patients with low AGL expressing bladder tumors in the near term. To address this need, we carried out a whole genome transcription analysis using Affymetrix Human Genome U219 Arrays in human bladder cancer cells depleted of AGL. We focused on genes upregulated in response to diminished tumor AGL expression which in turn may both drive tumor growth and be potential therapeutic targets. We found that increased mRNA expression of Hyaluronic Acid (HA) Synthase 2 and HA synthesis were found to drive tumor growth in bladder cancers with low AGL. We further showed that inhibition of HA synthesis is a potential therapeutic strategy for bladder tumors with low AGL expression.

MATERIAL AND METHODS

Cell line and Biochemical Reagents

UMUC3 and T24T control and AGL depleted human bladder cancer cells were, cultured and used as described(4). MGHU4 human bladder cancer cells were a generous gift from Dr. Fradet and AGL knockdown in these achieved using shRNA TRCN0000035082 (Sigma-Aldrich) designated as shAGL1. These three bladder cancer cell lines were chosen

for the study because they show an induction in growth with AGL loss, hence serve as good model cell lines to study AGL biology in bladder cancer. Stable AGL knockdown in UMUC3 was achieved using a second shRNA TRCN0000035080 (Sigma-Aldrich) designated as shAGL2. Bladder cell lines hTERT and TRT-HU1 were generous gifts from Drs. Adam(6) and Knowles respectively and AGL knockdown was achieved using shAGL1 above. Stable HAS2 knockdown was achieved in T24T cells with and without stable knockdown of AGL under neomycin resistance with shRNA TRCN0000432805 (Sigma-Aldrich). MISSION® pLKO.1-puro or pLKO.1-neo non-mammalian shRNA control plasmid DNA (SHC002, Sigma-Aldrich) was used as control for the gene knockdown experiments. 4-Methylumbelliferone (4-MU, cat. # M1508-10G) was obtained from Sigma-Aldrich. HA (cat. # GLR001) was obtained from R&D systems (Minneapolis, MN). siRNA sequences 5′-GCTGCTTATATTGTTGGCTTT-3′ (first) and 5′-GGTTTGTGATTCAGACACT-3′ (second) were used at a concentration of 50nM to knockdown HAS2 for different experiments. siGENOME SMARTpool siRNAs were used to knockdown RRAGD (M-016120-01-0005) and TULP3 (M-011415-01-0005) at a conc of 20nM. siRNA's were purchased from Dharmacon (Lafayette, CO) and transfected using Lipofectamine RNAiMAX (Invitrogen) using manufacturer instructions. Human bladder cancer cell lines MGHU4, T24T, and UMUC3 were authenticated by the University of Colorado PPSR core using an Applied Biosystems Profiler Plus Kit which analyzed 9 STR loci (Life Technologies 4303326). After authentication cells were frozen within 1-2 weeks. Vials of cells were resuscitated less than 2 months prior to being used in experiments in this study.

Microarray and Statistical Analysis

UMUC3 cells transduced with non-targeted shRNA or shRNA specific to AGL (shAGL1 described above) were grown to sub confluence followed by standard mRNA isolation. Whole genome transcription analysis was done using Affymetrix Human Genome U219 Arrays (GEO accession no. GSE73456). Differentially expressed genes between AGL-depleted and control cells were identified with false discovery rate (FDR) of 2% using linear models implemented in the *limma* package in R (Supp. Table 1). Patient microarray and clinicopathologic information is shown in Supp. Table 2. Raw microarray data were processed and normalized by the Robust Multi-array Average algorithm implemented in the *affy* package in R. In case of multiple probe sets for one gene, the probe with the highest mean expression across all samples was selected to represent the gene's expression. Gene expression differences between two groups of samples (tumor vs. normal, high grade vs. low grade, and muscle invasive (MI) vs. non-muscle invasive tumors (NMI)) were tested by Wilcoxon rank sum tests. Associations of numerical (continuous) and categorical gene expression with survival were examined by Cox proportional hazards models and logrank tests. For multivariable survival analysis, a full model included AGL and HAS2 expression and three clinically relevant variables (grade, T stage and N stage). A best model (i.e. final model) with the lowest Akaike information criterion (AIC) was also generated through forward step-wise addition of these five variables. Data from *in vitro* and *in vivo* experiments were analyzed by 2-tailed Student t-test with unequal variances. Error bars denote standard deviation or standard error of the mean as indicated.

PCR and Western Blot

HAS1-3, RRAGD, TULP3 mRNA expression was determined by the ΔΔCT method (4) with GAPDH as control for human bladder cancer cell lines and 18S for murine bladder tissues. Expression was normalized to control-treated cells to determine gene expression in AGL knockdown cells, and to shCTL-neo/shCTL-puro cells for expression of HAS2 in HAS2 and AGL dual stable knockdown T24T cells. HAS1 primer: forward 5′-TGTGCTGCGTCTGTTCTAC-3′ reverse 5′-CTCTGGTTCATGGTGACTAGC-3′; HAS 2 primer: forward 5′-TCCCGGTGAGACAGATGAGT-3′ reverse 5′-GGCTGGGTCAAGCATAGTGT-3′; HAS3 primer: forward 5′-TCCCTCTACTCCCTCCTCTAT-3′ reverse 5′-CTGAACAGGTCCTGGCAATAA-3′; RRAGD primer: forward 5′-TCTGGACTTCAGTGACCCCT-3′ reverse 5′-TGAATAGACGACTTGCCGCT-3′; TULP3 primer: forward 5′-TTTGGACGTGTGGCAGATGA-3′ reverse 5′-CGCCAGCTTACTGTCAAAGC-3′; VCAN primer: forward 5′-TTCAACCTTAATAGTAACCCATGC-3′ reverse 5′-AAGGTAGGCTGACTTTTCCAGAG-3′; EREG primer: forward 5′-GCATCTATCTGGTGGACATGAG-3′ reverse 5′-AAGGTTGGTGGACGGTTAAA-3′; GAPDH primer: forward 5′-TCTTTTGCGTCGCCAGCCGA-3′ reverse 5′-ACCAGGCGCCCAATACGACC-3′; 18S primer: forward 5′-TAATTCCGATAACGAACGAGAC-3′ reverse 5′-TCTAAGGGCATCACAGACC-3′ were used for the RT-PCR experiments. The HAS1-3 primers mentioned above were used for both human and mice tissues. Antibodies used for westerns were anti-AGL (Abgent, San Diego, CA) and anti- α tubulin (Calbiochem, San Diego, CA). HRP (Cell Signaling) labeled mouse or rabbit secondary antibodies were used chemiluminescence using ECL (Pierce, Rockford, IL).

Hyaluronic Acid (HA) ELISA

Fresh media is applied 72hrs after HAS2 siRNA transfection in control and AGL knockdown cells followed by HA analysis by ELISA 24 hrs later. T24T cells with stable knockdown of AGL and HAS2 are plated and fresh media is added when cells are 60–65% confluent followed by HA ELISA 24 hrs later. Cells with and without AGL are grown to a confluence of 60–65% followed by fresh media addition with different 4MU concentrations to evaluate the impact of 4MU on HA synthesis and secretion after 24hrs. HA ELISA was conducted as per manufacturer instructions using TECO® HA ELISA kit.

Anchorage Dependent and Independent Proliferation and Xenograft Tumor Growth

Anchorage dependent and independent proliferation was measured as before(4). For xenograft experiments, 4-week old athymic NCr- nu/nu mice were obtained from either National Cancer Institute (NCI-Frederick, Frederick, MD) or Charles Rivers Laboratory (Wilmington, MA). Cells with and without AGL depletion were transfected with control or HAS2 siRNA. 48 hrs after transfection, cells were injected subcutaneously in the left and right flanks of mice; UMUC3 at 25×10^3 cells/site, a cell concentration at which cells have very low tumor take(4) and T24T cells with dual stable knockdown of AGL and HAS2 at 10^5 cells/site. To study the effect of 4MU on the growth of bladder cancer xenografts, UMUC3 and T24T cells with AGL depletion were injected subcutaneously in mice at $2X10^6$

and 10^5 cells/site. Once the tumors were palpable mice were treated with 4MU at 200 mg/kg daily (except weekend). Tumors were measured and tumor volume calculated as described(4).

RESULTS

Expression profiling of human bladder cancer cells in response to AGL depletion

UMUC3 cells were transduced with control shRNA or shRNA specific for AGL and whole genome transcription analysis performed revealing 137 differentially regulated probes at FDR of 2% representing 100 genes (Supp. Table 1). To improve the likelihood of identifying therapeutic targets we focused on genes upregulated with AGL loss and found 38 genes (Figure 1A, Supp. Figure 1). Expression of these were evaluated in human tumors (Supp. Table 2) for evidence of association with 4 clinicopathologic variables: malignancy (tumor vs. normal), stage, grade and patient survival. Seven of 38 genes (SEMA3A, HAS2, RRAGD, VCAN, EREG, TULP3 and UCHL1) had a statistically significant positive correlation with at least 3 of these 4 variables using a numerical (continuous) input of the gene expression level avoiding the requirement of empirical cutoffs (Figure 1A). Interestingly, none had been implicated in AGL biology or function. Ubiquitin carboxyl-terminal esterase L1 (UCHL1) and semaphorin 3A (SEMA3A) have been shown to be tumor suppressors in other tumor models (10–13) hence were not investigated further here.

In contrast, we showed Versican (VCAN) and epiregulin (EREG) contribute to bladder tumor growth(14, 15) and while hyaluronic acid synthase 2 (HAS2) has been implicated in regulating bladder tumor growth, its role had yet to be explored in detail(16, 17). Finally, Tubby like protein 3 (TULP3) and RAS related GTP binding D (RRAGD) had never been implicated in bladder cancer (18–20). Next, we carried out qRT-PCR for mRNA expression of HAS2, RRAGD, VCAN, EREG and TULP3 in UMUC3 cells with and without AGL depletion using two different shRNA constructs (shAGL1 and shAGL2) and in T24T cells with AGL depletion to confirm and generalize the whole genome transcription analysis. HAS2, RRAGD, VCAN and TULP3 were confirmed to be expressed at higher levels in cells with AGL depletion compared to controls in both cell lines (Figure 1B, Supp. Figure 2). VCAN and HAS2 mRNA overexpression was most prominent with AGL loss when both shAGL constructs and both the bladder cancer cell lines were considered (Figure 1B, Supp. Figure 2). HAS2 is responsible for HA synthesis suggesting that HA synthesis and signaling is upregulated with AGL loss thus providing a viable therapeutic option.

AGL loss drives *in vitro* bladder cancer cell growth in part via HAS2

To determine the impact of these validated genes in bladder cancer growth as a function of AGL expression, we used siRNA to knockdown these genes (HAS2, RRAGD and TUPL3) (Figure 2A, B, C) in conjunction with AGL depletion using two different shRNAs (shAGL1 and shAGL2). We did not evaluate VCAN since it had already been implicated in bladder cancer(14). Of the three, HAS2 depletion had the most marked reduction of proliferation in UMUC3 cells with AGL loss (Figure 2D, E, F and Supp. Figure 3). A second siRNA against HAS2 was also able to significantly reduce the proliferation of UMUC3 cells with AGL loss (Supp. Figure 4A) confirming the dependence of bladder cancer cells with AGL loss on

HAS2. Given these results and that HAS2 encodes a protein that is part of a signaling pathway(22, 23) with therapeutic potential we selected this gene for in depth investigation.

siRNA driven knockdown of HAS2 in UMUC3 cells completely inhibited the increase in anchorage independent growth observed with AGL loss (Figure 2G). Next we evaluated the impact on anchorage dependent and independent growth of stable HAS2 depletion in T24T cells with stable AGL knockdown (Figure 2H) and observed that loss of HAS2 specifically inhibited the anchorage dependent and independent growth of T24T cells with AGL loss (Figure 2I, J). High HAS2 mRNA expression was also observed in bladder cancer cell line MGHU4 with AGL loss (Supp. Figure 4B). HAS2 siRNA depletion also reduced proliferation of MGHU4 bladder cancer cells with AGL loss (Supp. Figure 4C). These data indicate HAS2 is an important effector of cancer cell growth driven by AGL loss.

HAS2 is a member of a 3 gene family. To determine specificity, we evaluated the mRNA expression of HAS1 and 3 as a function of AGL depletion. HAS1 mRNA was undetectable in UMUC3 while HAS3 mRNA expression was not changed with AGL loss (Figure 3A). Next we investigated if HAS2 expression increases with loss of AGL in immortalized but non-transformed human urothelial cells. AGL depletion in two independent TERT immortalized cell lines led to increased HAS2 expression (Figure 3B). Furthermore, we examined the bladders obtained from AGL knockout mice developed to study GSDIII(24) and observed that HAS2 is overexpressed in these compared to littermate controls whereas expression of the other HAS isoforms was reduced (Figure 3C). These results reveal that HAS2 expression is induced by AGL loss in both mouse and human urothelium as well as in human bladder cancer cells, and that AGL loss drives *in vitro* bladder cancer cell growth in part via HAS2. This data suggests the AGL-HAS2 regulatory axis is of significant biological importance in normal physiology and cancer.

Hyaluronic acid synthesis by HAS2 drives bladder cancer growth

HA synthesized by HAS can contribute to tumor growth(21, 22). Hence we asked whether HA synthesis by HAS2 is increased with AGL loss. Interestingly, UMUC3, T24T and MGHU4 cells secrete more HA in response to AGL depletion and this increase disappears when HAS2 is depleted (Figure 4A, Supp. Figure 5A, B). To evaluate the importance of HA in promoting growth of bladder cancer cells with low AGL we treated UMUC3 and T24T shCTL and shAGL cells with 4MU, an inhibitor of HA synthesis(25, 26). 4MU treatment reduced HA in the cell media of shAGL cells to near control levels when used at a concentration of 400μM or higher (Figure 4B). 4MU at a concentration of 400μM also inhibited proliferation of UMUC3 and T24T cells depleted of AGL to a similar degree to knockdown of HAS2 (Figure 4C, Supp. Figure 5C). Next we treated UMUC3 and T24T with HA and 4MU together and observed a partial rescue of the 4MU growth inhibitory effect by HA (Figure 4D, Supp. Figure 5D). While this data is consistent with other reports which show that commercially available HA can only partially rescue such growth inhibitory effects(27, 28) it also suggests that 4MU mediated growth inhibition is due to inhibition of HA synthesis and signaling.

HA synthesis blockade slows bladder cancer xenograft growth *in vivo*

We investigated if reduced HAS2 mediated HA synthesis can slow xenograft tumor growth. We knocked down HAS2 in UMUC3 shAGL1 cells. Cells were then injected subcutaneously into nude mice and tumor growth monitored (4). UMUC3 cells with both AGL and HAS2 depletion had reduced tumor growth compared to cells with only AGL loss and UMUC3 control cells +/- HAS2 expression (Figure 5A). A similar observation was made in T24T cells (Figure 5B). Interestingly, loss of HAS2 had minimal growth inhibitory effect on control cells (shCTL) supporting the notion that HAS2/HA mediate the increased growth seen with AGL loss.

To evaluate the potential of HA synthesis inhibition as a therapeutic option for bladder cancer patients with reduced tumor AGL expression we investigated the impact of 4MU on the *in vivo* growth of UMUC3 and T24T bladder cancer cell lines with stable depletion of AGL. All mice had palpable tumors after 10 days they were either injected intraperitoneally 5 days/wk with 4MU at a dose of 200 mg/kg or vehicle control. 4MU inhibited the xenograft growth of UMUC3 and T24T (Figure 5C, D) indicating that 4MU or similar drugs can be potential therapeutic options for bladder cancers with low AGL expression.

The relevance of AGL and HAS2 mRNA expression in human bladder cancer

The role of HAS2 mRNA as a predictor of bladder patient outcome is unclear(16). We detected that high HAS2 mRNA expression is observed in high grade (HG) and muscle invasive (MI) bladder tumors compared to low grade (LG) and non-muscle invasive tumors (NMI) (Figure 6A) across two independent patient datasets. Next we evaluated how the mRNA expression of HAS2 correlates with that of AGL in bladder cancer patients across 5 independent bladder cancer patient datasets comprising of 552 patients (Supp. Table 2). We observed that AGL mRNA expression has a negative correlation with HAS2 mRNA expression in all datasets with statistical significance in 4 of 5 datasets (Figure 6B). When patients were divided into MI and NMI forms of the disease, the correlation findings between AGL and HAS2 were similar (*data not shown*). The statistically significant negative correlations were also observed in advanced (T3/T4 and high grade) cancer in 3 of the datasets and in localized (Ta/T1 and low grade) cancer in 1 dataset (Supp. Table 3). These data provide clinical support and further confirmation of biological relevance of the observation made in human bladder cancer cells and in AGL knockout mice that low or absent AGL leads to high HAS2 expression.

We also explored if expression of AGL and HAS2 can stratify patient outcome. The primary objective here was to determine if such expression levels could eventually be used to identify the optimal patient cohort who may be enrolled in future clinical trials with inhibitors of HA signaling. The secondary objective was to lead credence to the hypothesis that AGL affects tumor biology by HAS2 as well as other effectors such as SHMT2(4). Our earlier analysis (Figure 1A) using a numerical (continuous) input of the gene expression shows that high HAS2 expression is associated with poor overall patient survival in Kim *et al* (29) dataset with hazard ration (HR) 1.55 (p=0.036). In contrast, high AGL expression is associated with an HR=0.33 (p=0.013) using continuous input denoting its tumor growth suppressive features. Next we showed the impact of these on overall survival using Kaplan

Meier analysis of patients split into two groups. AGL high expressing were those patients in the top 70% while low expressors were those in the bottom 30% (Figure 6Ci). In the case of HAS2 the cutpoint was top 40% vs. bottom 60% (Figure 6Cii). In both cases, survival was significantly stratified by these variables, supporting the more general continuous analysis above. When analyzing AGL and HAS2 expression in a multivariable survival model that included 3 clinically relevant variables (grade, stage, and nodal status), AGL provided marginally significant, independent prognostic value (HR=0.62, p=0.069; the full model in Supp. Table 4). In a final model that selected a concise and optimal set of variables via forward step-wise addition of variables, AGL was selected over stage and was an independent prognostic factor (HR=0.60, p=0.044; Supp. Table 4).

Next we examined the utility of combining AGL and HAS2 expression in stratifying bladder patient outcome. Using continuous input of AGL/HAS2 expression level ratio, we observed that bladder cancer patients with high ratios had the better overall survival HR = 0.01 (p = 0.001). Kaplan-Meier survival using the same cutoffs as for individual variables above also revealed a significant stratification of survival but with a somewhat better HR of 2.55 (Figure 6Ciii). Importantly, both analyses indicated that combining these two variables enhanced the magnitude of the stratification as measured by the HR compared to using either variable alone. However, the combined AGL and HAS2 expression was not significant in multivariable survival analyses (Supp. Table 5). Taken together, AGL and HAS2 mRNA expression can stratify patient overall survival in both univariable and multivariable models while combining expression of these enhances such stratification in a univariable fashion.

DISCUSSION

Our study is the first to establish HAS2 mediated HA synthesis as a driver of growth of bladder cancer cells with low AGL and provide preclinical rationale for personalized targeting of HAS2/HA signaling in patients with low AGL expressing tumors. Several findings of our study are intriguing and merit discussion. The HAS enzyme family consists of three isoforms implicated in HA synthesis. While all are implicated in tumor formation and progression in a variety of studies(21, 23), only HAS2 expression is increased in both human bladder cancer and immortalized urothelial cell lines with loss of AGL, as well as in bladders of AGL knockout mice. This observed relationship between AGL and HAS2 expression in immortalized human and benign murine urothelium suggests AGL regulates biology beyond that linked to glycogen storage since HAS2 is the most common HAS isoform expressed by mammalian tissues and HA synthesized by HAS2 is important for numerous cellular functions.

In addition to HAS2, another interesting finding links HA to AGL biology. HA is a high molecular weight polysaccharide and core component of the extracellular matrix(20–22). UDP-GluUA and UDP-GlcNAc are precursors of HA and HAS substrates(20, 30). In fact, HA synthesis consumes large quantities of these and their concentration can be rate limiting for HA synthesis. While the content of these UDP sugars varies between cell types and responds to metabolic changes(20, 30), glucose is known to be the major starting substrate for these. Interestingly, our studies in bladder cancer cells revealed that loss of AGL

increases glucose uptake and utilization and this promotes growth(4). In addition, high cytosolic glucose can activate the PKC pathway which in turn induces HAS expression, increasing HA synthesis(31, 32).

HAS2 expression is transcriptionally regulated by other signaling pathways in addition to glucose. While it is unclear what directly drives HAS2 gene overexpression in response to AGL loss several mechanisms can be envisioned. First, it is conceivable that HAS2 expression and HA synthesis are both driven by enhanced glucose driven by loss of AGL, as discussed above. With loss of AGL, glucose is channeled into HA as a major end metabolite, and that HA imparts pro-tumorigenic signaling. Second, as yet undiscovered proteins with which AGL interacts can be positive regulators of HAS2, with the model being that when AGL is abundant, these are kept in an inactive form by either sequestration or posttranslational modification for example.

Analysis of AGL and HAS2 expression in human bladder cancer revealed these are negatively correlated supporting and generalizing the *in vitro* findings on human cell lines and tissues from transgenic mice. High HAS2 mRNA expression is observed in HG and MI bladder tumors and is associated with poor bladder cancer patient outcome. While HAS1 and HAS3 have both been implicated in bladder cancer biology(16, 17, 27, 33), neither mRNA is induced by AGL depletion suggesting that these genes are not responsible for the aggressive biology associated with AGL loss. Analysis showed that patients with low AGL and high HAS2 expression had poor overall survival. The greater hazard rate in the combined analysis compared to AGL and HAS2 alone indicates that expression of HAS2 in combination with AGL may be a better predictor of patient outcome and response to therapy with HA synthesis inhibitors than either alone. Furthermore, taking the correlation of AGL and HAS2 expression in both experimental systems and patient tumors together with the enhanced stratification of patient outcome by both variables leads us to speculate that AGL and HAS2 have both related and independent effects on tumor biology. This notion is consistent with data showing that loss of AGL also drives growth signals via SHMT2(4) in addition to HAS2.

Finally, here we show that an increase in HA synthesis driven by HAS2 is responsible for *in vitro* and *in vivo* growth of bladder cancer cells with AGL loss. RNAi targeting of HAS2 and inhibition of HA with 4MU in AGL depleted cells both suppressed the growth of bladder cancer cells *in vitro* and *in vivo* indicating that the tumor-promoting function of HAS2 is dependent on its enzymatic activity and that HA synthesis in turn leads to tumor growth in response to AGL depletion.

4MU is a well known inhibitor of HA synthesis(25, 34). It is a non-toxic drug which is also used as a dietary supplement in Europe and Asia to improve liver health(34). Recent studies have shown that 4MU plays an important role in inhibiting tumor growth and metastasis. In prostate cancer 4MU plays a critical role in cancer prevention and also reduces primary tumor growth and metastasis(34). However the role of 4MU in bladder cancer prevention and in treating primary and metastatic bladder cancer is unknown. Ours is the first study to show that 4MU can inhibit xenograft growth of bladder cancer cells that have lost AGL. We plan to use chemical carcinogenesis to induce bladder cancer in AGL knockout mice to

study the role 4MU in bladder cancer prevention, primary tumor growth and metastasis. We propose that 4MU will be a viable therapeutic option for “personalized” treatment of bladder cancer patients with low AGL expression.

Supplementary Material

Refer to Web version on PubMed Central for supplementary material.

Acknowledgments

Funding: Supported in part by National Institutes of Health grant CA143971 to DT, the Bladder Cancer Advocacy Network (BCAN) Young Investigator Award and the Cancer League of Colorado, research grant to SG, and the National Institutes of Health Ruth L. Kirschstein F32 National Research Service Award (NRSA) F32CA189735 to CRL.

Abbreviations

AGL	amylo-alpha-1-6-glucosidase-4-alpha-glucanotransferase
HAS1/2/3	hyaluronic acid synthase 1/2/3
TULP3	tubby like protein 3
RRAGD	RAS related GTP binding D
VCAN	versican
EREG	epiregulin
SEMA3A	semaphorin 3A
UCHL1	Ubiquitin carboxyl-terminal esterase L1
HA	hyaluronic acid
4MU	4-Methylumbelliferone
FBS	fetal bovine serum
GSDIII	glycogen storage disease type III
PYG	glycogen phosphorylase
DMEM	Dulbecco’s modified Eagle’s medium
MEM	modified Eagle’s medium
NaP	sodium pyruvate

References

1. Murray, Robert KDKG.; Mayes, Peter A.; Rodwell, Victor W. Harper’s Illustrated Biochemistry. 26. McGraw Hill; 2003.
2. Kishnani PS, Austin SL, Arn P, Bali DS, Boney A, Case LE, et al. Glycogen storage disease type III diagnosis and management guidelines. Genet Med. 2010; 12:446–63. [PubMed: 20631546]
3. Shen J, Bao Y, Liu HM, Lee P, Leonard JV, Chen YT. Mutations in exon 3 of the glycogen debranching enzyme gene are associated with glycogen storage disease type III that is differentially expressed in liver and muscle. J Clin Invest. 1996; 98:352–7. [PubMed: 8755644]

4. Guin S, Pollard C, Ru Y, Ritterson Lew C, Duex JE, Dancik G, et al. Role in tumor growth of a glycogen debranching enzyme lost in glycogen storage disease. J Natl Cancer Inst. 2014; 106(5)
5. Lin CW, Lin JC, Prout GR Jr. Establishment and characterization of four human bladder tumor cell lines and sublines with different degrees of malignancy. Cancer Res. 1985; 45:5070–9. [PubMed: 4027986]
6. Kim J, Ji M, DiDonato JA, Rackley RR, Kuang M, Sadhukhan PC, et al. An hTERT-immortalized human urothelial cell line that responds to anti-proliferative factor. In Vitro Cell Dev Biol Anim. 2011; 47:2–9. [PubMed: 21136194]
7. Chapman EJ, Hurst CD, Pitt E, Chambers P, Aveyard JS, Knowles MA. Expression of hTERT immortalises normal human urothelial cells without inactivation of the p16/Rb pathway. Oncogene. 2006; 25:5037–45. [PubMed: 16619045]
8. Smyth, GK. Limma: linear models for microarray data. New York: Springer; 2005.
9. Gautier L, Cope L, Bolstad BM, Irizarry RA. affy--analysis of Affymetrix GeneChip data at the probe level. Bioinformatics. 2004; 20:307–15. [PubMed: 14960456]
10. Jin C, Yu W, Lou X, Zhou F, Han X, Zhao N, et al. UCHL1 Is a Putative Tumor Suppressor in Ovarian Cancer Cells and Contributes to Cisplatin Resistance. J Cancer. 2013; 4:662–70. [PubMed: 24155778]
11. Tang C, Gao X, Liu H, Jiang T, Zhai X. Decreased expression of SEMA3A is associated with poor prognosis in gastric carcinoma. Int J Clin Exp Pathol. 2014; 7:4782–94. [PubMed: 25197349]
12. Trifa F, Karray-Chouayekh S, Jmaa ZB, Jmal E, Khabir A, Sellami-Boudawara T, et al. Frequent CpG methylation of ubiquitin carboxyl-terminal hydrolase 1 (UCHL1) in sporadic and hereditary Tunisian breast cancer patients: clinical significance. Med Oncol. 2013; 30:418. [PubMed: 23315218]
13. Zhou H, Wu A, Fu W, Lv Z, Zhang Z. Significance of semaphorin-3A and MMP-14 protein expression in non-small cell lung cancer. Oncol Lett. 2014; 7:1395–400. [PubMed: 24765144]
14. Said N, Sanchez-Carbayo M, Smith SC, Theodorescu D. RhoGDI2 suppresses lung metastasis in mice by reducing tumor versican expression and macrophage infiltration. J Clin Invest. 2012; 122:1503–18. [PubMed: 22406535]
15. Nicholson BE, Frierson HF, Conaway MR, Seraj JM, Harding MA, Hampton GM, et al. Profiling the evolution of human metastatic bladder cancer. Cancer Res. 2004; 64:7813–21. [PubMed: 15520187]
16. Kramer MW, Escudero DO, Lokeshwar SD, Golshani R, Ekwenna OO, Acosta K, et al. Association of hyaluronic acid family members (HAS1, HAS2, and HYAL-1) with bladder cancer diagnosis and prognosis. Cancer. 2011; 117:1197–209. [PubMed: 20960509]
17. Okegawa T, Ushio K, Imai M, Morimoto M, Hara T. Orphan nuclear receptor HNF4G promotes bladder cancer growth and invasion through the regulation of the hyaluronan synthase 2 gene. Oncogenesis. 2013; 2:e58. [PubMed: 23896584]
18. Sancak Y, Bar-Peled L, Zoncu R, Markhard AL, Nada S, Sabatini DM. Ragulator-Rag complex targets mTORC1 to the lysosomal surface and is necessary for its activation by amino acids. Cell. 2010; 141:290–303. [PubMed: 20381137]
19. Mukhopadhyay S, Jackson PK. The tubby family proteins. Genome Biol. 2011; 12:225. [PubMed: 21722349]
20. Tammi RH, Passi AG, Rilla K, Karousou E, Vigetti D, Makkonen K, et al. Transcriptional and post-translational regulation of hyaluronan synthesis. FEBS J. 2011; 278:1419–28. [PubMed: 21362137]
21. Adamia S, Maxwell CA, Pilarski LM. Hyaluronan and hyaluronan synthases: potential therapeutic targets in cancer. Curr Drug Targets Cardiovasc Haematol Disord. 2005; 5:3–14. [PubMed: 15720220]
22. Karbownik MS, Nowak JZ. Hyaluronan: towards novel anti-cancer therapeutics. Pharmacol Rep. 2013; 65:1056–74. [PubMed: 24399703]
23. Lokeshwar VB, Mirza S, Jordan A. Targeting hyaluronic Acid family for cancer chemoprevention and therapy. Adv Cancer Res. 2014; 123:35–65. [PubMed: 25081525]

24. Pagliarani S, Lucchiari S, Ulzi G, Violano R, Ripolone M, Bordoni A, et al. Glycogen storage disease type III: A novel Agl knockout mouse model. Biochim Biophys Acta. 2014; 1842:2318–28. [PubMed: 25092169]

25. Edward M, Quinn JA, Pasonen-Seppanen SM, McCann BA, Tammi RH. 4-Methylumbelliferone inhibits tumour cell growth and the activation of stromal hyaluronan synthesis by melanoma cell-derived factors. Br J Dermatol. 2010; 162:1224–32. [PubMed: 20163414]

26. Piccioni F, Malvicini M, Garcia MG, Rodriguez A, Atorrasagasti C, Kippes N, et al. Antitumor effects of hyaluronic acid inhibitor 4-methylumbelliferone in an orthotopic hepatocellular carcinoma model in mice. Glycobiology. 2012; 22:400–10. [PubMed: 22038477]

27. Golshani R, Lopez L, Estrella V, Kramer M, Iida N, Lokeshwar VB. Hyaluronic acid synthase-1 expression regulates bladder cancer growth, invasion, and angiogenesis through CD44. Cancer Res. 2008; 68:483–91. [PubMed: 18199543]

28. Li Y, Li L, Brown TJ, Heldin P. Silencing of hyaluronan synthase 2 suppresses the malignant phenotype of invasive breast cancer cells. Int J Cancer. 2007; 120:2557–67. [PubMed: 17315194]

29. Kim WJ, Kim EJ, Kim SK, Kim YJ, Ha YS, Jeong P, et al. Predictive value of progression-related gene classifier in primary non-muscle invasive bladder cancer. Mol Cancer. 2010; 9:3. [PubMed: 20059769]

30. Vigetti D, Passi A. Hyaluronan synthases posttranslational regulation in cancer. Adv Cancer Res. 2014; 123:95–119. [PubMed: 25081527]

31. Hascall VC, Wang A, Tammi M, Oikari S, Tammi R, Passi A, et al. The dynamic metabolism of hyaluronan regulates the cytosolic concentration of UDP-GlcNAc. Matrix Biol. 2014; 35:14–7. [PubMed: 24486448]

32. Wang A, de la Motte C, Lauer M, Hascall V. Hyaluronan matrices in pathobiological processes. FEBS J. 2011; 278:1412–8. [PubMed: 21362136]

33. di Martino E, Kelly G, Roulson JA, Knowles MA. Alteration of cell-cell and cell-matrix adhesion in urothelial cells: an oncogenic mechanism for mutant FGFR3. Mol Cancer Res. 2015; 13:138–48. [PubMed: 25223521]

34. Yates TJ, Lopez LE, Lokeshwar SD, Ortiz N, Kallifatidis G, Jordan A, et al. Dietary supplement 4-methylumbelliferone: an effective chemopreventive and therapeutic agent for prostate cancer. J Natl Cancer Inst. 2015; 107(7)

STATEMENT OF TRANSLATIONAL RELEVANCE

Loss of Amylo-alpha-1-6-glucosidase-4-alpha-glucanotransferase (AGL) drives bladder cancer growth. Low AGL expression predicts poor patient outcome. Currently no specific therapeutically tractable targets/pathways exist that could be used to treat patients with low AGL expressing bladder tumors. To address this issue we carried out a transcriptome analysis in human bladder cancer cells with and without AGL expression to identify pro-tumorigenic pathways upregulated with AGL loss. We identified and validated that hyaluronic acid (HA) synthase 2 (HAS2) expression and subsequent HA synthesis is upregulated with AGL loss. We validated that HAS2 and consequent HA synthesis drive tumor growth and that genetic and pharmacologic inhibition of these respectively is a viable therapeutic option in xenograft models. We further established that bladder cancer patients with low AGL expression and high HAS2 expression have poor outcome. Together, this data provide preclinical evidence for personalized targeting of HAS2/HA signaling in patients with low AGL expressing tumors.

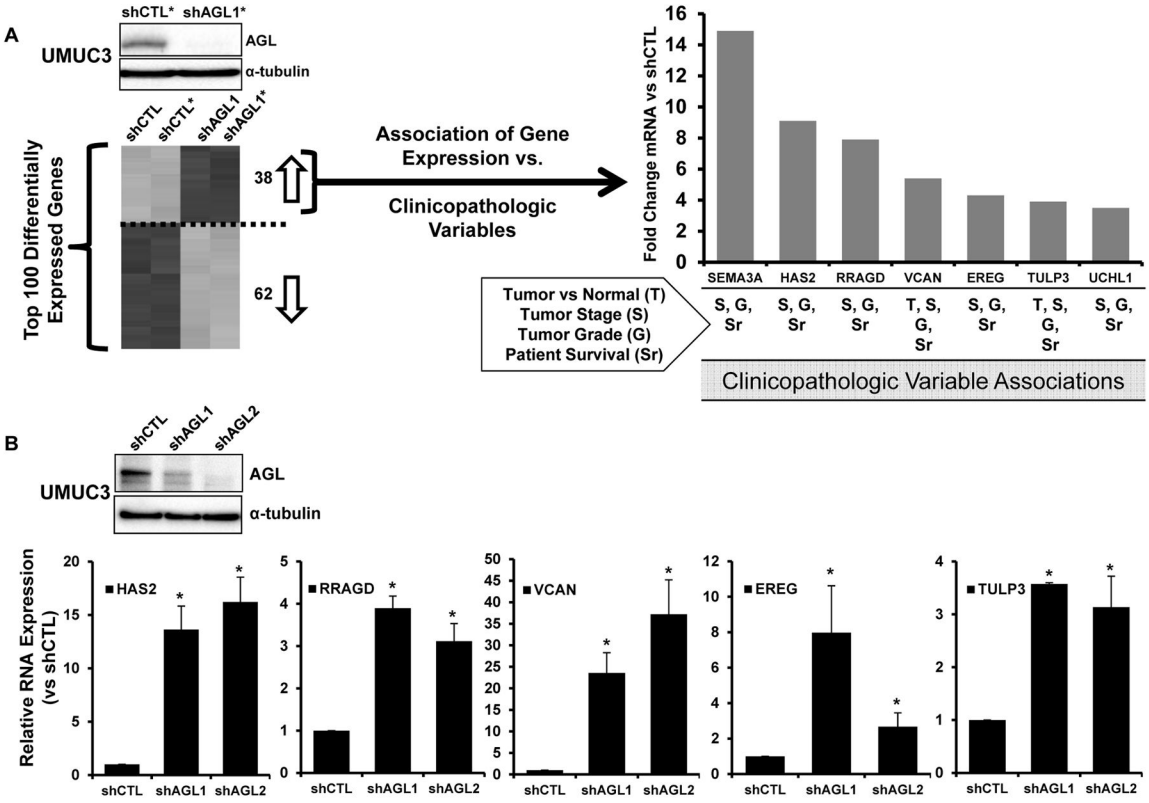

Figure 1. Transcriptional profiling of human bladder cells as a function of AGL followed by evaluation of gene expression in clinical specimens

A. Diagram of heatmap and biomarker analysis carried out on differentially regulated genes with shRNA mediated AGL depletion. *Representative western blot insert of one of two samples used for expression profiling. 38 of the top 100 (Supp. Table 1) differentially expressed genes were upregulated with AGL loss and were examined for association of their expression with clinicopathologic variables such as malignancy (tumor vs normal), high tumor stage, high tumor grade and patient survival in bladder cancer patients described in Supp. Table 2. Bar graph of microarray mRNA expression (Fold over UMUC3 shCTL) of 7 of 38 genes that had positive correlation with at least 3 of 4 clinicopathologic variables (indicated below graph). **B.** Quantitative reverse transcriptase polymerase chain reaction (qRT-PCR) for HAS2, RRAGD, VCAN, EREG and TULP3 in UMUC3 cells with (shCTL) or without AGL (shAGL1 and shAGL2; AGL knocked down with two different shRNA constructs as described in **Materials and Methods**) (n=3). AGL knockdown was validated by western blot (inset). Results are shown as mean ± SD, *p<0.05 by Student's t-test.

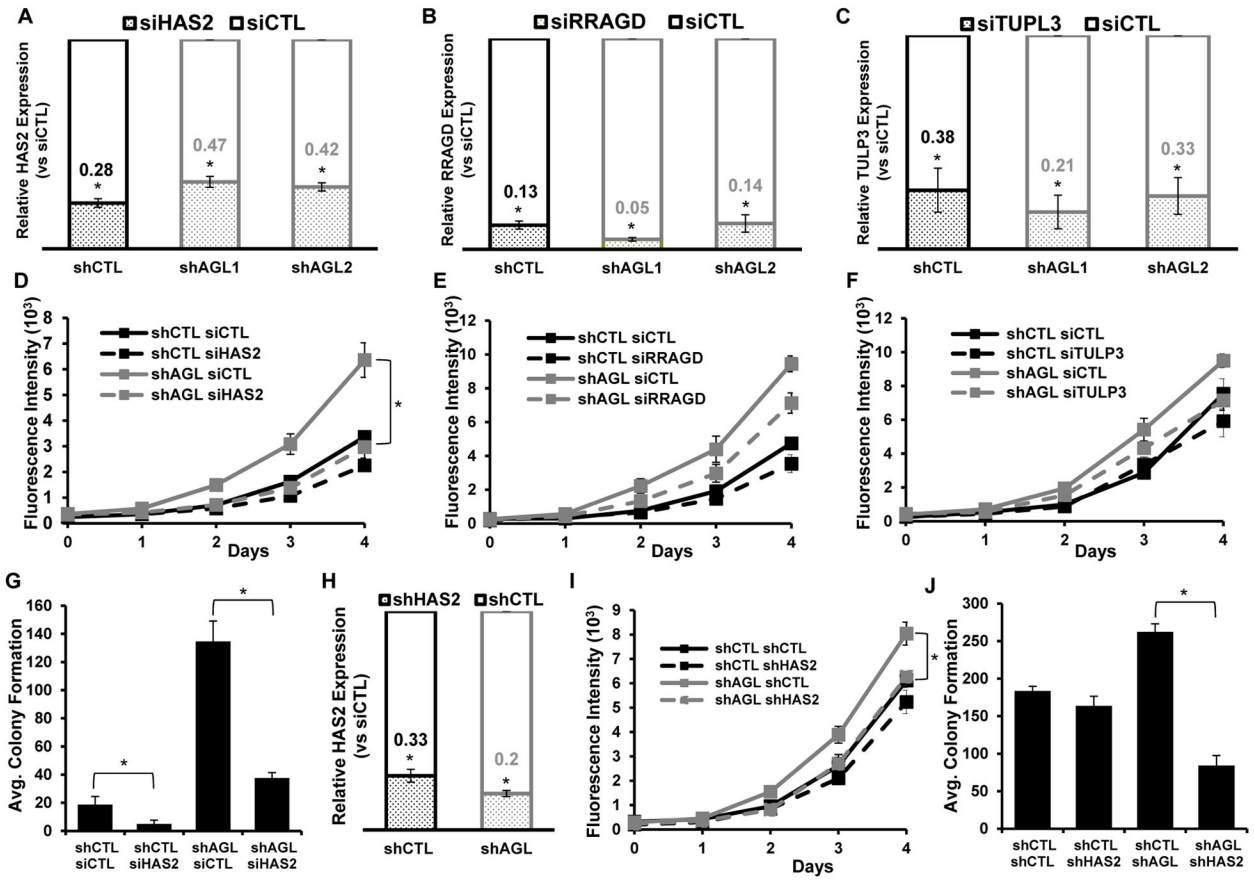

Figure 2. HAS2 is a driver of growth of bladder tumors with low AGL expression

A, B, C. qRT-PCR demonstrating efficacy of HAS2, RRAGD or TULP3 depletion in UMUC3 control (shCTL) and AGL knockdown (shAGL 1 and shAGL 2) cells. Cells were plated and 24hrs later transfected with scrambled or directed siRNA against specific genes. Details of siRNA used are in **Materials and Methods**. Cells were harvested at 72hrs for mRNA followed by qRT-PCR analysis (n=3). **D, E, F.** 48 hrs after UMUC3 shCTL and shAGL1 were transfected with various siRNAs, they were plated for monolayer growth (n-6) in 96-welled plate (10^3 cells/well) for 5 days followed by Cyquant assay (shAGL1=shAGL in figure). **G.** 48 hrs after UMUC3 shCTL and shAGL1 were transfected with siRNA against HAS2 they were plated in agar for evaluation of anchorage independent growth (15×10^3 cells/well) in 6 well plate (n=3) (shAGL1=shAGL in figure). **H.** qRT-PCR for HAS2 in T24T cells with dual stable knockdown of AGL (shAGL1) and HAS2 (n=3) (shAGL1=shAGL in figure). **I, J.** Impact of HAS2 depletion on monolayer (n=6) and anchorage independent (n=3) growth in T24T cells with (shAGL1) and without (shCTL) AGL depletion. 10^3 and $15X10^3$ cells were plated in 96 well plates and 6 well plate for **I.** monolayer growth and **J.** agar growth (shAGL1=shAGL figure). Results are shown as mean ±SD, *p<0.05 by Student's t-test.

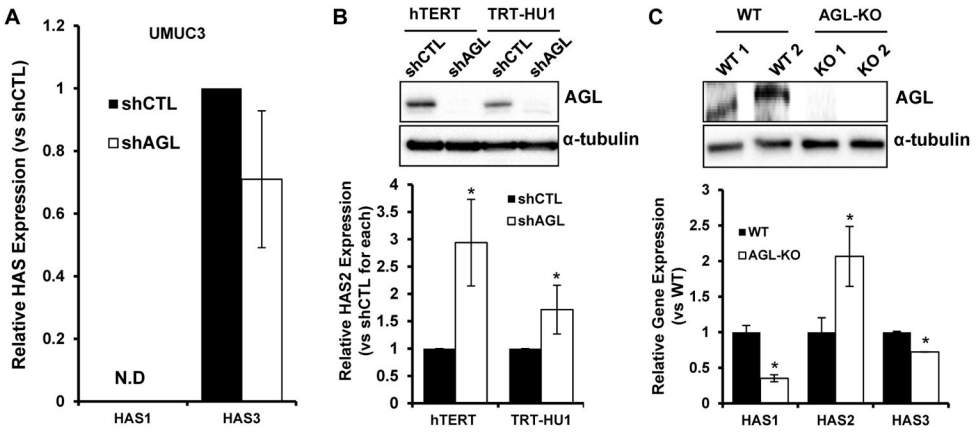

Figure 3. AGL and HAS2 expression are inversely correlated in immortalized and normal urothelium

A. qRT-PCR analysis for HAS isoforms HAS1 and HAS3 with AGL knockdown using shAGL1 shRNA construct (n=3) (shAGL1=shAGL in figure), N.D. not detectable. **B.** qRT-PCR for HAS2 in immortalized but non-transformed human urothelial cell lines with AGL knockdown using shAGL1 shRNA construct (n=3). AGL knockdown was validated by western blot (shAGL1=shAGL inset). **C.** qRT-PCR analysis on bladders of wild-type (WT) and AGL knockout (KO) mice for HAS1-3 (n=3). AGL knockdown was validated by western blot (inset) in two individual murine bladders (WT 1, 2 and KO 1, 2) of WT and AGL-KO mice respectively. Results are shown as mean ± SD, *p<0.05 by Student's t-test.

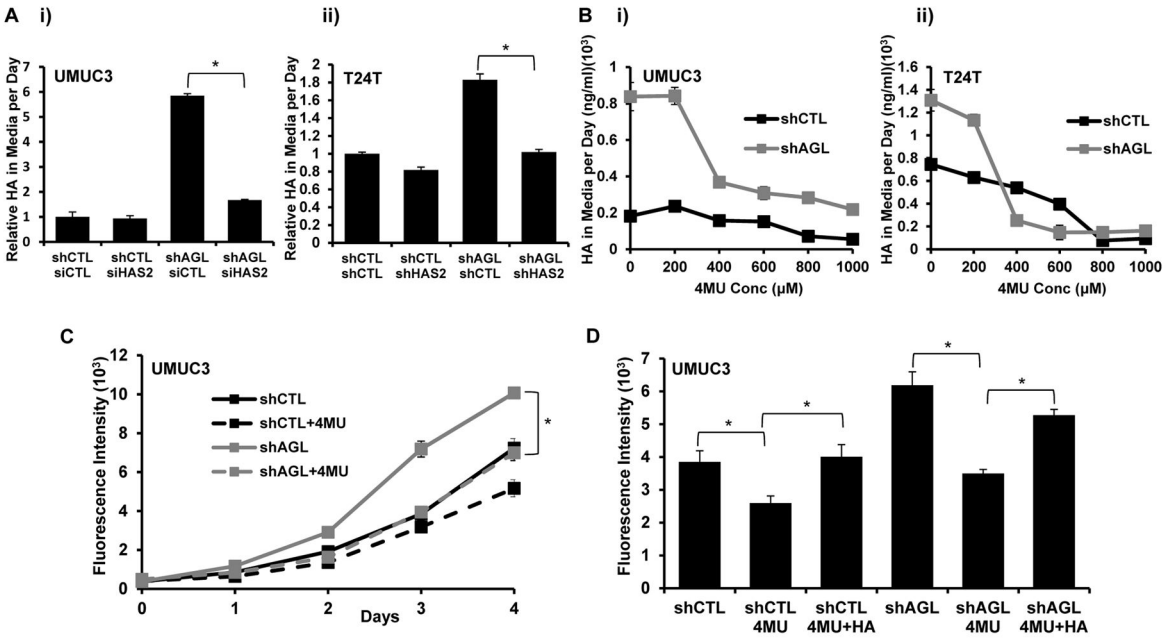

Figure 4. HAS2 driven HA production drives growth of bladder cancer cells with low AGL

A. HA in cell culture media of UMUC3 and T24T cells with loss of HAS2 in cells with (shAGL1) and without (shCTL) AGL depletion. **i)** UMUC3 (shCTL and shAGL1) cells were plated followed by siRNA induced knockdown of HAS2. Fresh media was added 48 hrs after transfection followed by HA ELISA on the media 24 hrs later (n=3). **ii)** T24T cells with dual stable knockdown of AGL and HAS2 were plated, 24 hrs later media was changed and 24 hrs after that, HA analysis carried out (n=3) (shAGL1=shAGL in figure). **B.** UMUC3 **i)** and T24T **ii)** cells with (shAGL1) and without (shCTL) AGL loss were plated. Next day media with varying concentrations of 4MU was added and cells incubated for 24 hrs after which HA analysis on media was carried out (n=3) (shAGL1=shAGL in figure). **C.** UMUC3 (shCTL and shAGL1) cells (10^3) were plated in 96 well plates (n=6) with 400μM 4MU for 5 days followed by monolayer growth assay (shAGL1=shAGL in figure). **D.** UMUC3 (shCTL and shAGL1) cells (10^3) were plated in 96 wells plates (n=6) with 400μM 4MU or 4MU +HA for monolayer growth assay (shAGL1=shAGL in figure). Results are shown as mean ± SD, *p<0.05 by Student's t-test.

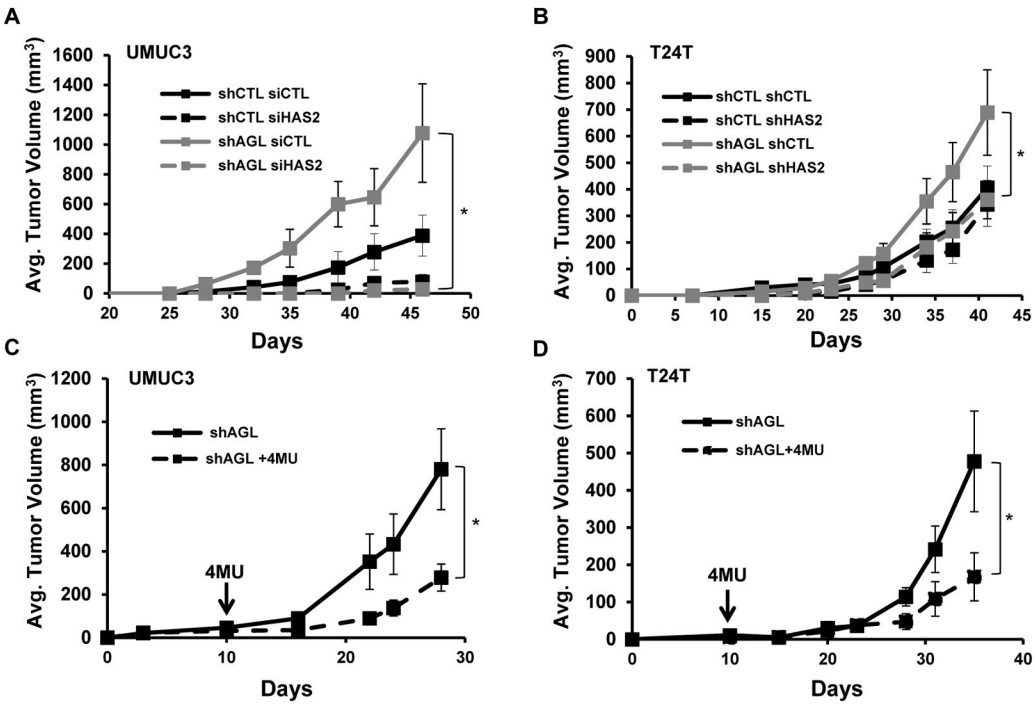

Figure 5. HA synthesis blockade slows bladder cancer xenograft growth

A. UMUC3 (shCTL and shAGL1) cells transfected with scrambled (siCTL) or HAS2 siRNA (siHAS2) were injected subcutaneously in the left and right flank of nu/nu mice (25×10^3 cells/site). Tumor volume was measured in a total of 10 injection sites per condition (shAGL1=shAGL in figure). **B.** T24T cells with stable knockdown of both AGL and HAS2 were injected subcutaneously in the left and right flank of nu/nu mice (10^5cells/site). Tumor volume was measured in a total of 10 injection sites (shAGL1=shAGL in figure). **C, D** UMUC3 and T24T AGL knockdown cells (shAGL1) were injected subcutaneously in the left and right flank of nu/nu mice (2×10^6 and 10^5 cells/site for UMUC3 and T24T respectively. Tumors were palpable in all mice at 10 days at which point mice were randomly assigned to intraperitoneal treatment with vehicle control or 4MU (200 mg/Kg daily). shAGL1=shAGL in figure. Results are shown as mean ± SEM, *p<0.05 by Student's t-test.

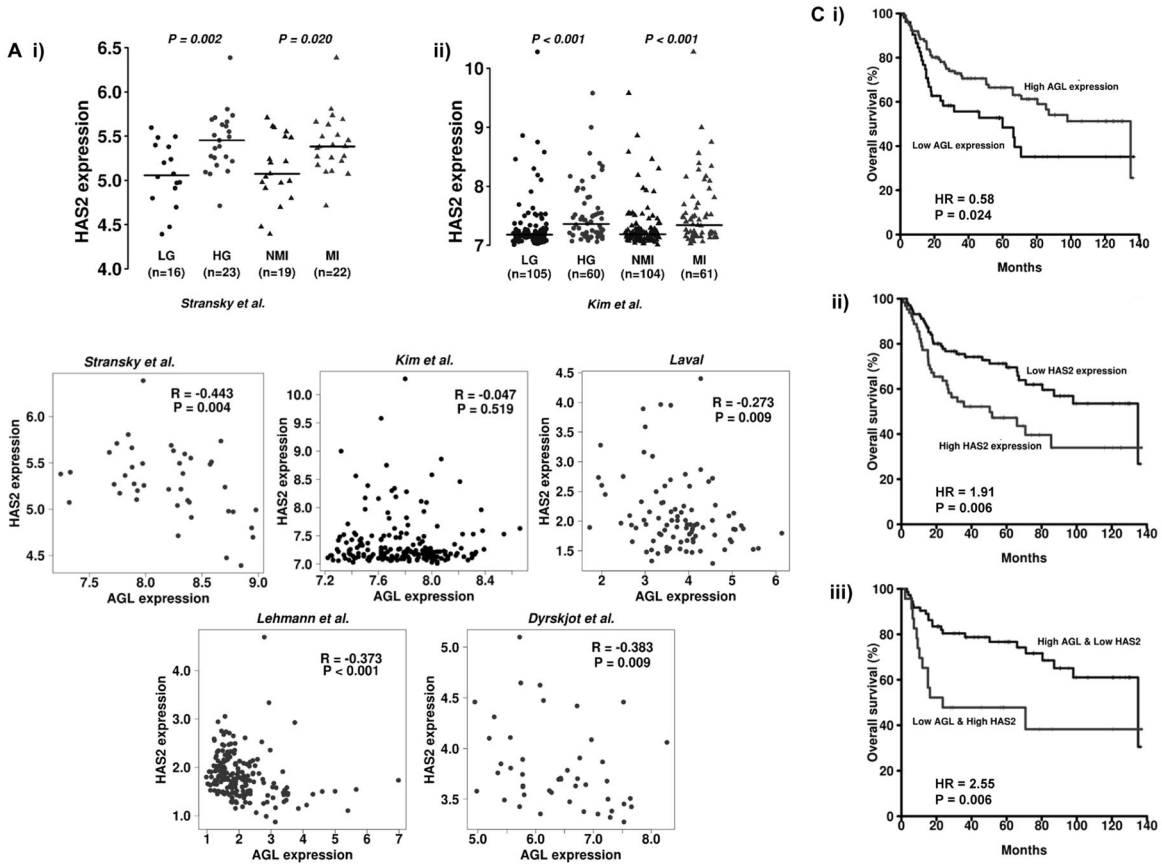

Figure 6. Relationship of HAS2 and AGL mRNA to clinicopathologic variables in human bladder cancer

A. HAS2 mRNA expression in (**i**) high grade (HG) and (**ii**) muscle invasive (MI) bladder tumors compared to low grade (LG) and non-muscle invasive (NMI) bladder tumors in two independent patient datasets Stransky *et al.* and Kim *et al.* (Supp. Table 2). **B.** Spearman correlations of AGL expression with the expression of HAS2 in bladder cancer tumors (total n=552) across 5 independent patient datasets (Supp. Table 2). Scatter plots in red and black for statistically significant and insignificant data respectively. **C.** Kaplan Meier analysis of categorized (high/low) mRNA levels of **i)** AGL; **ii)** HAS2 and **iii)** AGL and HAS2 and overall survival in the Kim *et al.*(29) bladder patient dataset. Hazard Rates (HR) and P values (logrank) are shown. High- and low-expression groups were determined by an optimal cutoff that gave the best p-value and was selected from nine different percentiles (from 10^{th} to 90^{th}).